Int. J. Electrochem. Sci., 6 **(2011)** 847 - 859

International Journal of
ELECTROCHEMICAL
SCIENCE
www.electrochemsci.org

Alkaloids Extract from *Palicourea guianensis* Plant as Corrosion Inhibitor for C38 Steel in 1 M Hydrochloric Acid Medium

M. Lebrini, F. Robert[*], *C. Roos*

Laboratoire Matériaux et Molécules en Milieu Amazonien, UAG-UMR ECOFOG,
Campus Trou Biran, Cayenne 97337, French Guiana.
[*]E-mail: florent.robert@guyane.univ-ag.fr

Received: 5 January 2011 / *Accepted:* 3 February 2011 / *Published:* 1 March 2011

Corrosion inhibition effect of alkaloids extract from *Palicourea guianensis* plant (AEPG) on C38 steel in 1 M HCl medium has been investigated by potentiodynamic polarization and electrochemical impedance spectroscopy. The polarization studies showed that AEPG acts as mixed-type inhibitor. The electrochemical impedance spectroscopy showed that the charge transfer resistance increases and the double layer capacitance decreases on increasing plant extract concentration. The inhibition efficiency of the extract obtained from impedance and polarization measurements was in a good agreement and was found to increase with increasing concentration of the extract. Inhibition efficiency of 89% was achieved with 100 mg L^{-1} of AEPG at 25 °C. The obtained results showed that, the *Palicourea guianensis* extract could serve as an effective inhibitor for the corrosion of steel in acid media. The adsorption of AEPG obeys the Langmuir adsorption isotherm.

Keywords: *Palicourea guianensis*, corrosion inhibitors, C38 steel, acidic media, adsorption

1. INTRODUCTION

Steel and steel-based alloys of different grades steel are extensively used in numerous applications where acid solutions are widely applied such as industrial acid pickling, industrial acid cleaning and oil-well acidizing. These service domains lead to certain corrosion of exposed surfaces of the metal. It is a general consensus that the best method to protect the metal deployed in these corrosive environments is to insert corrosion inhibitors. To this end, the use of organic and inorganic substances to inhibit corrosion of metals is well established [1–7]. Recently, plant extracts have again become important as an environmentally acceptable, readily available and renewable source for a wide

range of needed inhibitors. Several researchers studied the effect of natural products as corrosion inhibitors in different media [8–20]. In addition, plant products are low-cost, readily available, and renewable sources of materials. In previous work [11,12], the inhibition effect of alkaloids extract from *Oxandra asbeckii* and *Annona squamosa* plants on the corrosion of C38 steel in 1 M hydrochloric acid solution has been investigated by potentiodynamic polarization and electrochemical impedance spectroscopy. Alkaloids extract from these plants was found to reduce the corrosion of steel and that the organic compounds in the extracts establish their inhibition via adsorption of their molecules on the metal surface forming a protective barrier.

The present report continues to focus on the broadening application of plant extracts for metallic corrosion control and reports on the inhibiting effect of the alkaloids extract from *Palicourea guianensis* plant (AEPG) on C38 steel corrosion in acidic solution.

2. EXPERIMENTAL

2.1. Electrode and solution

Corrosion tests have been carried out on electrodes cut from sheets of C38 steel. Steel strips containing 0.36 wt% C, 0.66 wt% Mn, 0.27 wt% Si, 0.02 wt% S, 0.015 wt% P, 0.21 wt% Cr, 0.02 wt% Mo, 0.22 wt% Cu, 0.06 wt% Al and the remainder iron. The specimens were embedded in epoxy resin leaving a working area of 0.78 cm^2. The working surface was subsequently ground with 180 and 1200 grit grinding papers, cleaned by distilled water and ethanol. The solutions (1 M HCl) were prepared by dilution of an analytical reagent grade 33% HCl with doubly distilled water. All the tests were performed at ambient temperature (25 °C).

2.2. Preparation of plant extract

Extraction — Dried ground leaves of *Palicourea guianensis* were treated with alkaline solutions (NH_4OH 5%). The alkalized raw material was extracted with dichloromethane (3x200 mL). The extract was collected by filtration and the combined dichloromethane fractions were washed with water (2x200 mL). Then, the organic layer was extracted three times with diluted HCl. The combined aqueous fractions were washed with dichloromethane (3x80 mL) and the pH of the aqueous solution was adjusted to 9 with aqueous solution (NH_4OH 25%). This aqueous layer was extracted with dichloromethane (3x100 mL) and the combined organic layers were washed with distilled water (2x100 mL), dried over Na_2SO_4 and collected by filtration. The solvent was removed under reduced pressure, and the alkaloids residue was obtained [21]. After collecting alkaloids extract, the remaining extract was analyzed by HPLC (Fig.1a). It contains over 3 major peaks along with many small peaks indicating presence of more than 30 compounds. The small peaks may be attributed to the compounds present in small quantities as well as disintegrated major compounds. After that, the crude extract was submitted to preparative HPLC on silica gel impregnated with Octadecyl (C18) and eluted in acetonitril/water gradient, yielding fractions which were analyzed by HPLC. It's found that these

fractions contained a mixture of many compounds (Fig. 1b and 1c, representative example). Similar results were found for the others isolated fractions. Since retention time of compounds is close to each other and it is very difficult to separate them, hence the total alkaloids extract from *Palicourea guianensis* plant was used as such for corrosion inhibition studies. The concentration range of alkaloids extract from *Palicourea guianensis* plant employed was 5 – 100 mg L^{-1}.

HPLC system — The HPLC separations were performed on a Supelco Discovery HS PEG column (25 cm x 21.2 mm, 5 lm) using a Waters system equipped with a W600 pump and a W2996 photodiode array absorbance detector. The samples were injected manually through a Rheodyne injector and the flow rate was 1 ml/min.

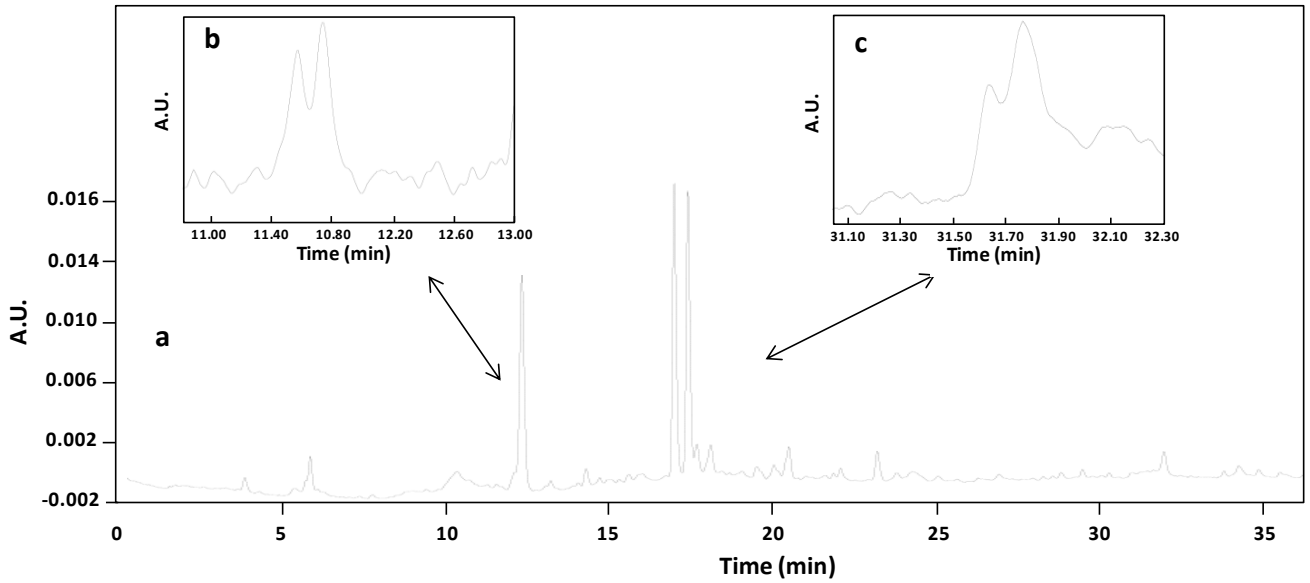

Figure 1. HPLC spectroscopy spectra of total alkaloids extract from *Palicourea guianensis;* (a) total alkaloids extract, (b) and (c) isolated fractions at different retention time.

2.3. Electrochemical measurements

Electrochemical measurements, including potentiodynamic polarization curves and electrochemical impedance spectroscopy (EIS) were performed in a three-electrode cell. The C38 steel specimen was used as the working electrode, a platinum wire as the counter electrode and a saturated calomel electrode (SCE) as the reference electrode. Before each Tafel and EIS experiments, the electrode was allowed to corrode freely and its open-circuit potential (OCP) was recorded as a function of time during 3 h, the time necessary to reach a quasi-stationary value for the open-circuit potential. This steady-state OCP corresponds to the corrosion potential (E_{corr}) of the working electrode.

The anodic and cathodic polarisation curves were recorded by a constant sweep rate of 20 mV min^{-1}. Electrochemical impedance spectroscopy (EIS) measurements were carried out, using ac signals of amplitude 5 mV peak to peak at different conditions in the frequency range of 100 kHz to 10 mHz. Electrochemical measurements were performed through a VSP electrochemical measurement system (Bio-Logic). The above procedures were repeated for each concentration of the two tested inhibitors.

The Tafel and EIS data were analysed using graphing and analyzing impedance software, version EC-Lab V9.97.

3. RESULTS AND DISCUSSION

3.1. Polarisation curves

Fig. 2 illustrates the cathodic and anodic polarization curves recorded for C38 in 1 M HCl solutions without and with various concentrations of AEPG. Electrochemical corrosion kinetic parameters obtained by Tafel extrapolation method are given in Table 1. As it can be seen from Fig. 2, the anodic and cathodic reactions are affected by the inhibitor, indicating that AEPG acts as mixed-type inhibitors. The addition of AEPG to HCl solution, therefore reduces the anodic dissolution of iron and also retards the cathodic hydrogen evolution reaction, see Eqs. (1) and (2).

$$\mathrm{Fe} = \mathrm{Fe}^{2+} + 2\mathrm{e}^{-} \tag{1}$$

$$2\mathrm{H}^{+} + 2\mathrm{e}^{-} = \mathrm{H}_2 \tag{2}$$

The shapes of the polarization plots, in all cases, for HCl solutions containing inhibitor are not considerably different from those of free HCl solutions. The presence of the AEPG decreases the corrosion rate but does not change other aspects of the behaviour. This means that the AEPG do not modify the electrochemical reactions responsible for corrosion. as well, the absence of significant changes in the cathodic and anodic Tafel slopes in the presence of AEPG, see Table 1, indicates that the hydrogen evolution also the anodic metal dissolution reactions are slowed down by the surface blocking effect of the inhibitor. This indicates that the inhibitive action of the AEPG may be related to the adsorption of extract molecules on the electrode surface. It can be seen from the polarization results, Table 1, that the corrosion current density decreased noticeably with the increase in inhibitor concentration, due to increase in the blocked fraction of the electrode surface by adsorption. No definite shift in the corrosion potential (E_{corr}) is detected, although there was not a specific relation between E_{corr} and inhibitor concentrations. The polarization resistances (R_p) values were determined in the potential range ± 25 mV from the corrosion potential. It's found that the polarization resistance values increases with the increase in AEPG concentration. The inhibition efficiencies are calculated from the corrosion current density (Eq. (3)) and the polarization resistances (Eq. (4)). It's found that *IE*(%) increases with inhibitor concentration reaching a maximum value at 100 mg L^{-1}. The inhibition efficiencies calculated from the polarization resistances show the same trend as those obtained from the corrosion current (I_{corr}).

$$IE(\%) = \frac{I_{corr} - I_{corr(inh)}}{I_{corr}} \times 100 \tag{3}$$

where I_{corr} and $I_{corr(inh)}$ are the corrosion current densities obtained by extrapolation of the cathodic and anodic Tafel data from uninhibited and inhibited solutions, respectively.

$$IE(\%) = \frac{R_p - R_{p(inh)}}{R_p} \times 100 \quad (4)$$

where R_p and $R_{p(inh)}$ are the polarization resistances obtained in the potential range ±25 mV from the corrosion potential for inhibited and uninhibited solutions, respectively.

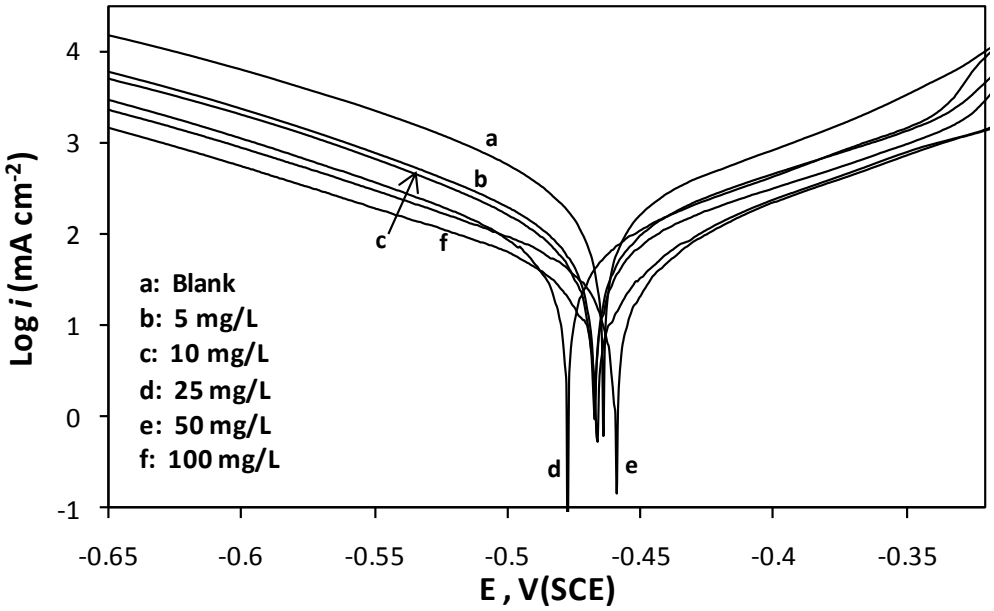

Figure 2. Polarisation curves for C38 steel in 1 M HCl containing different concentrations of AEPG.

Table 1. Polarization parameters and the corresponding inhibition efficiency for the corrosion of C38 steel in 1 M HCl containing different concentrations of AEPG at 25 °C.

Concentration mg L^{-1}	E_{corr} vs SCE	I_{corr}	b_a	b_c	R_p	IE Icorr	IE Rp
	(mV)	(μA cm^{-2})	(mV dec^{-1})	(mV dec^{-1})	(Ω cm^2)	(%)	(%)
1 M HCl	-463	232	89	105	76	—	—
5	-467	83	96	101	175	64	57
10	-467	53	75	107	249	77	69
25	-477	45	78	92	318	81	76
50	-460	32	87	98	453	86	83
100	-466	23	88	104	615	90	88

3.2. Electrochemical impedance spectroscopy (EIS)

The corrosion behaviour of C38 steel in HCl solution in the presence of AEPG was also investigated by the EIS method at 25 °C (Fig. 3). All the impedance spectra obtained for the corrosion of C38 steel in HCl solutions with inhibitor consist of two capacitive loops (two well-defined time-constants in the Bode-phase format on Fig. 4). The high-frequency (HF) loop, the smaller one that it can not be seen clearly, can be attributed to the film formation at the steel surface while the low-frequency (LF) loop, the larger one, can be attributed to the charge transfer reaction. Also, these impedance diagrams are not perfect semicircles which are related to the frequency dispersion as a result of the roughness and inhomogeneous of electrode surface [22–26]. Furthermore, it is apparent, from these plots that, the impedance response of C38 steel in uninhibited HCl solution has significantly changed after addition of AEPG in the corrosive solution. As a result, real axis intercepts at high and low frequencies in the presence of inhibitor are bigger than that in the absence of inhibitor (blank solution) and increases as the inhibitor concentration increases. This confirms that the impedance of inhibited substrate increases with the concentration of AEPG in 1 M HCl. The Figure 5 shows the equivalent circuit used to fit the impedance data, recorded for a C38 electrode 1 M HCl in the presence of different concentrations of AEPG. In this circuit, one can distinguish a high frequency (HF) part (CPE_f and R_f) representing the film formation at the steel surface and a low frequency (LF) part (CPE_{dl} and R_{ct}) attributed to the charge transfer reaction. A constant phase element (CPE) is substituted for the capacitive element to give a more accurate fit [27]. The constant phase element is composed of a component *A* and a coefficient *n*. The parameter *n* quantifies different physical phenomena like surface inhomogeneousness resulting from surface roughness and inhibitor adsorption. The main parameters deduced from the fit of Nyquist diagram for 1 M HCl medium containing various concentrations of AEPG are given in Table 2. In the same Table are shown also the calculated ″double layer capacitance″ values (C_{dl}), using the Eq. (3) [28–30]:

$$C_{dl} = (A.R_{ct}^{\ 1-n})^{1/n} \quad (3)$$

Where *A* is the CPE constant and *n* is a CPE exponent.

Additions of AEPG increases n_{dl} value indicating reduction of surface inhomogeneity due to the adsorption of plant extract molecules. Capacitance values decreases on increasing the AEPG concentration indicates reduction of charges accumulated in the double layer due to formation of adsorbed plant extract layer [17] Also, the value of the proportional factor A_{dl} of CPE varies in a regular manner with inhibitor concentration. The charge transfer resistances of double layer (R_{ct}) increases on increasing the AEPG concentration indicating that increase in concentration of plant extract decreases corrosion rate and increases corrosion inhibition. The parameters characterizing the film formation are determined with a poor accuracy because their loop is too small on the overall Nyquist diagram, see Table 2. It's found that, the R_f values show a marked tendency to increase with concentration following the similar variation of R_{ct}. The film capacitance values, determined by the same expression given in Eq. 3, decreased with concentration. Thus, the decrease of the film

capacitance values can be explained by the thickening of the film. The values of n_f lies between 0.737 and 0.781 indicate that the surface inhomogeneity, in the film formation process, was not more affected by increasing concentration. The A_f values are almost dependent of the concentration of the inhibitor. The A_f values decrease continuously with concentration and its values are much higher than that obtained for the charge transfer process. The inhibition efficiency (*IE*) is given by:

$$IE\,(\%) = [(R_p - R_p^0)/R_p] \times 100 \quad (4)$$

where R_p^0 and R_p are respectively polarization resistances in the absence and presence of alkaloids extract. R_p values are the sum of charge transfer (R_{ct}), and inhibitor film (R_f) resistance. The corrosion inhibition efficiencies, calculated using these values, are similar with the same calculated using polarization data. The maximum of corrosion inhibition efficiency of 89% was noticed for 100 mg L^{-1} plant extract.

The use of the natural products such as extracted compounds from leaves or seeds as corrosion inhibitors have been widely reported by several authors [16,17,19,31–34]. As an example, Table 3 reports the percentage inhibition efficiency for some plants extracts used as corrosion inhibitors in various acidic media and their optimum concentrations. The data obtained by a lot of natural products (Table 3) and our results (Tables 1 and 2) suggests that the plant extracts could serve as effective corrosion inhibitors. In addition, plant extracts are viewed as an incredibly rich source of naturally synthesized chemical compounds that can be extracted by simple procedures with low cost and are biodegradable in nature.

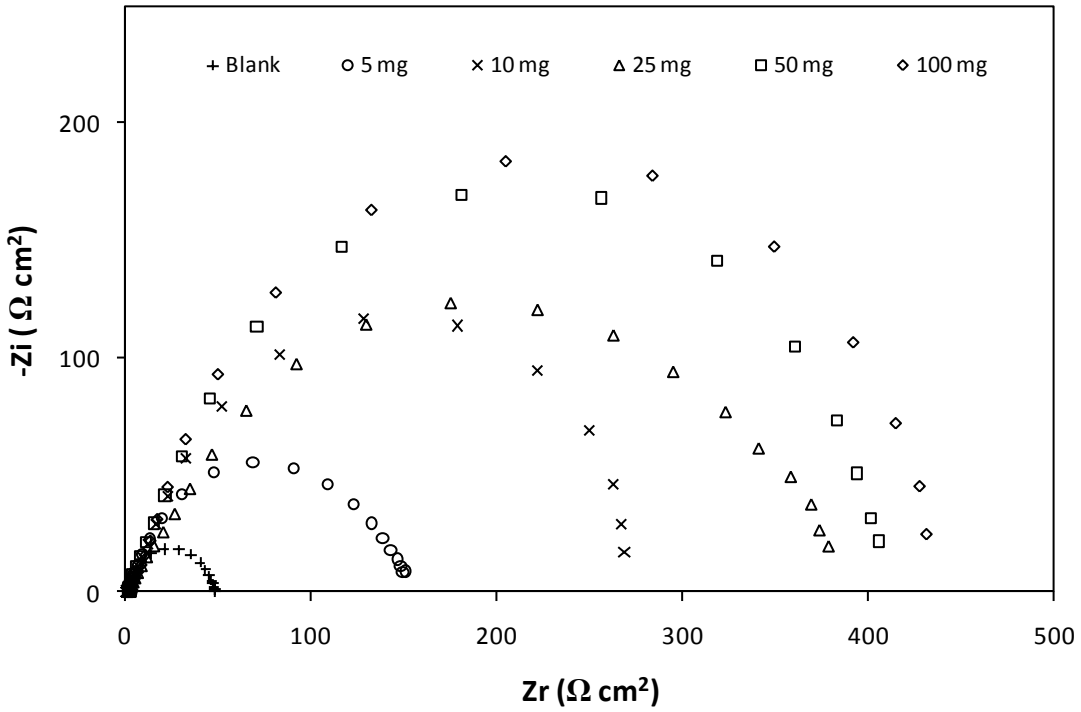

Figure 3. Nyquist plots for C38 steel in 1 M HCl in the absence and presence of different concentrations of AEPG.

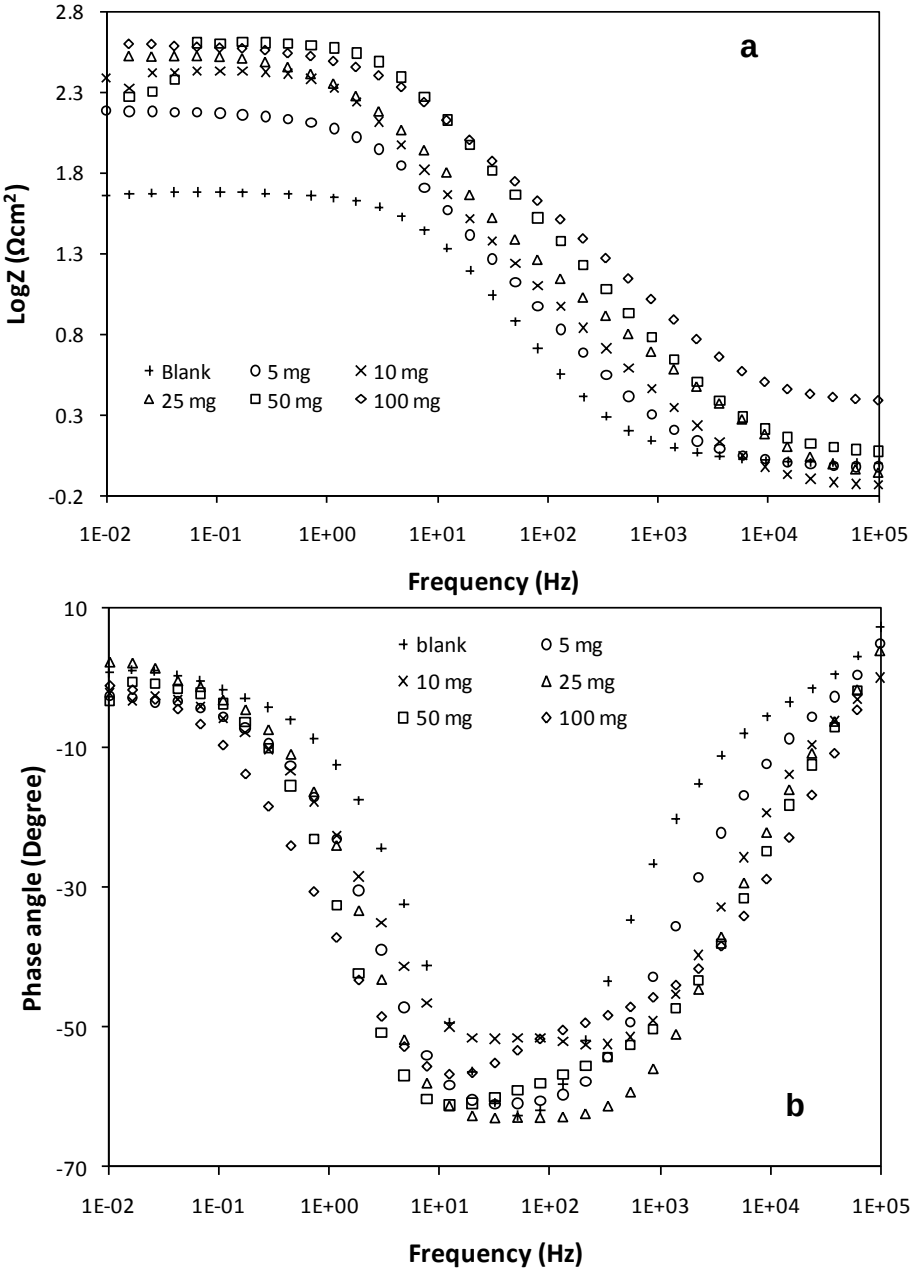

Figure 4. Bode plots, LogZ vs. freq (a) and phase angle vs. freq (b), for C38 steel in 1 M HCl in the absence and presence of different concentrations of AEPG.

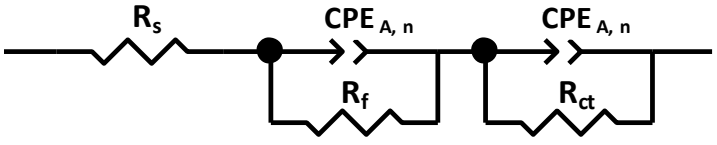

Figure 5. The equivalent circuit used to fit the impedance data, recorded for a C38 electrode 1 M HCl in the presence of different concentrations of AEPG.

Table 2. Values of the elements of equivalent circuit required for fitting the EIS for C38 steel in 1 M HCl in the absence and presence of different concentrations of AEPG and the corresponding inhibition efficiency.

Concentration (mg L^{-1})	R_f	10^4 A	n_f	C_{ct}	R_{ct}	10^4 A	n_{dl}	C_{ct}	IE
	(Ω cm^2)	(Ω^{-1} s^n cm^{-2})		(μF cm^{-2})	(Ω cm^2)	(Ω^{-1} s^n cm^{-2})		(μF cm^{-2})	(%)
1 M HCl	—	—	—	—	49 ± 0.02	9.50 ± 0.73	0.853 ± 0.014	546	—
AEPG									
5	2 ± 1.2	64.2 ± 15.6	0.737 ± 0.505	1357	153 ± 1.78	6.2 ± 0.16	0.862 ± 0.035	425	68
10	5 ± 4.1	48.7 ± 16.5	0.738 ± 0.558	1302	266 ± 0.42	5.1 ± 0.05	0.875 ± 0.021	383	82
25	7 ± 3.6	38.8 ± 10.5	0.758 ± 0.627	1227	386 ± 1.81	3.9 ± 0.01	0.888 ± 0.254	307	88
50	10 ± 4.8	29.1 ± 9.8	0.775 ± 0.561	1042	401 ± 2.83	2.5 ± 0.08	0.893 ± 0.023	190	88
100	21 ± 8.7	21.3 ± 9.7	0.781 ± 0.585	891	425 ± 3.58	2.1± 0.04	0.921 ± 0.015	171	89

Table 3. Critical concentration and percentage inhibition efficiency for different plants extracts

Natural Products	Optimum Concentration	Highest Inhibition Efficiency	Acidic Media	Metal Exposed
Lupine [16]	960 mg L^{-1} 640 mg L^{-1}	86.2% 86.2%	1 M H_2SO_4 2 M HCl	steel steel
Mango peel [17]	600 mg L^{-1}	91%	1 M HCl	carbon steel
Orange peel [17]	400 mg L^{-1}	95%	1 M HCl	carbon steel
Passion fruit peel [17]	500 mg L^{-1}	90%	1 M HCl	carbon steel
Cashew peel [17]	800 mg L^{-1}	80%	1 M HCl	carbon steel
Justicia gendarussa [19]	150 ppm	93%	1 M HCl	mild steel
Zenthoxylum alatum [31]	2400 ppm 2400 ppm	95% 91%	5% HCl 15% HCl	mild steel mild steel
Ricinus Communis leaves [32]	2500 v/v	96.96%	1 M HCl	mild steel
Chamaemelum mixtum L. [33]	7.56 g L^{-1}	90.2%	1 M H_2SO_4	steel
Nigella sativa L. [33]	1.14 g L^{-1}	87.2%	1 M H_2SO_4	steel
Cymbopogon proximus [33]	2.52 g L^{-1}	87.1%	1 M H_2SO_4	steel
Phaseolus vulgaris L. [33]	2.4 g L^{-1}	83.5%	1 M H_2SO_4	steel
Lasianthera africana [34]	0.5 g/L	94.23%	0.1 M H_2SO_4	mild steel

3.3. Adsorption Isotherm

Addition of extract molecules adsorbs on the metal surface and interaction between them can be described by adsorption isotherms [35]. The simplest, being the Langmuir isotherm, is based on assumption that all adsorption sites are equivalent and that particle binding occurs independently from nearby sites being occupied or not [36]. The data were tested graphically by fitting to various isotherms including Langmuir, Temkin and Frunkin (Figs. 6, 7 and 8). These models have been used

for other inhibitor systems [37]. According to these isotherms, θ is related to the inhibitor concentration C_{inh} via:

$$\frac{C_{\text{inh}}}{\theta} = \frac{1}{K} + C_{\text{inh}} \quad \text{(Langmuir isotherm)} \quad (5)$$

$$\left(\frac{\theta}{1-\theta}\right)\exp(-2a\theta) = KC_{\text{inh}} \quad \text{(Frumkin isotherm)} \quad (6)$$

$$\exp(-2a\theta) = KC_{\text{inh}} \quad \text{(Temkin isotherm)} \quad (7)$$

where "*K"* is the binding constant of the adsorption reaction and "*a*" is the lateral interaction term describing the molecular interactions in the adsorption layer and the heterogeneity of the surface. The θ values are calculated using impedance and polarization data. By far the best fit was obtained with the Langmuir isotherm (the strong correlation R^2 = 0.999 for both methods). The plots of C_{inh}/θ vs. C_{inh} yield a straight line. It indicates that the adsorbing AEPG species occupies typical adsorption site at the metal/solution interface. As can be seen by the good fit, AEPG as inhibitor, found to follow Langmuir adsorption isotherm.

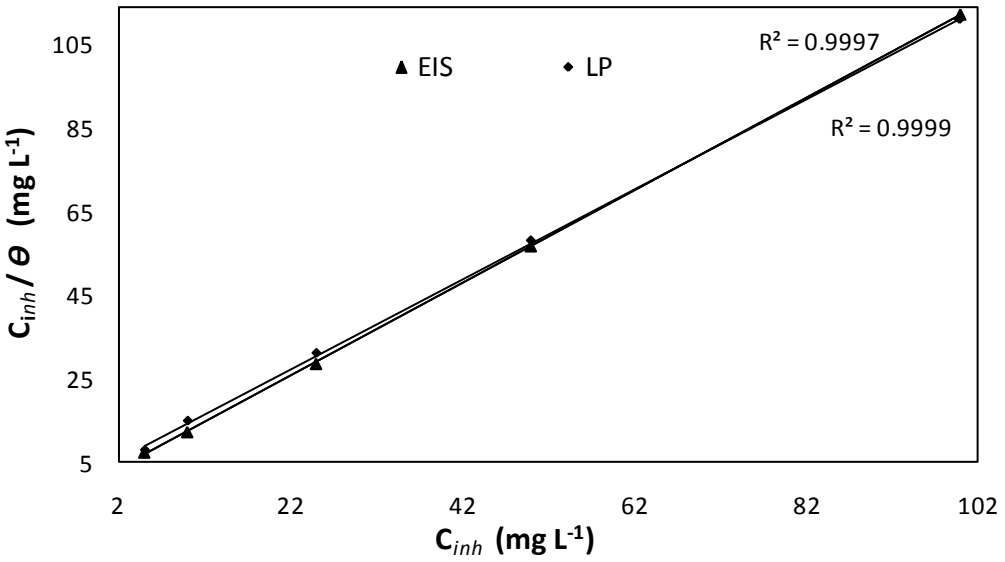

Figure 6. Langmuir adsorption plots for C38 steel in 1 M HCl containing different concentrations of AEPG.

The complex chemical compositions in this extract make it rather difficult to attribute the inhibiting action to a particular constituent or group of constituents. Alkaloid compounds have been shown to possess significant anticorrosion activity, which is principally based on their structural characteristics (nitrogen atoms, other groups, conjugation) [38]. Thus, the inhibitory effect observed in

polarization curves and electrochemical impedance diagrams results likely occurs via the adsorption of the alkaloid compounds present in the AEPG onto the steel surface. However, a synergistic or antagonistic effect of these molecules may play an important role on the inhibition efficiency of AEPG. It is very important to note that discussion of the adsorption behavior using natural product extracts as inhibitors in terms of thermodynamic parameters **(**such as the standard free energy of adsorption value (ΔG_{ads})) is not possible because the molecular mass of the extract components is not known. For example, there are a several alkaloid compounds in the extract. Some authors [16,17,19], in their study on acid corrosion with plant extract, noted the same limitation.

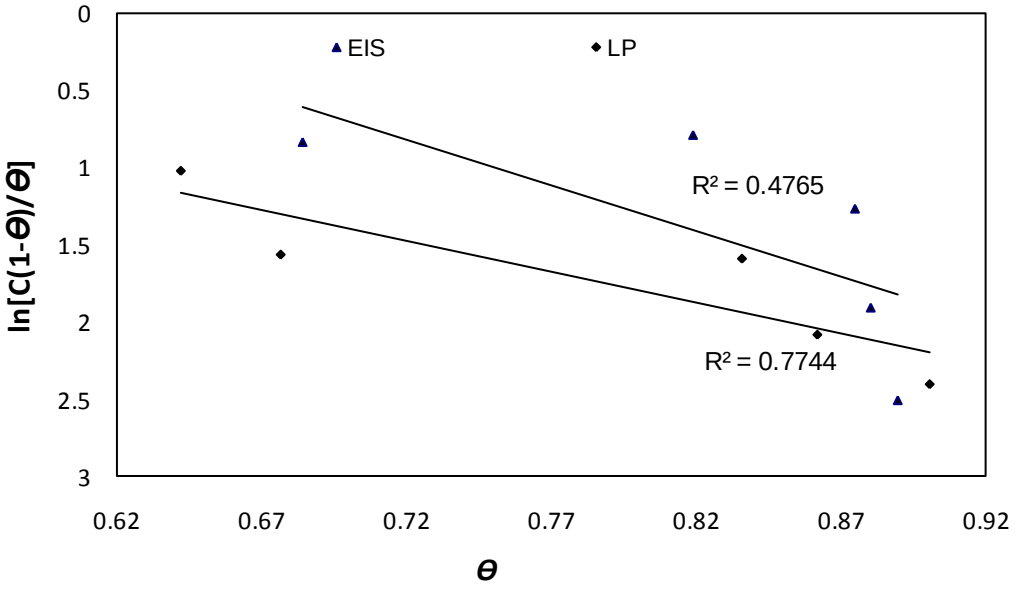

Figure 7. Frumkin adsorption plots for C38 steel in 1 M HCl containing different concentrations of AEPG.

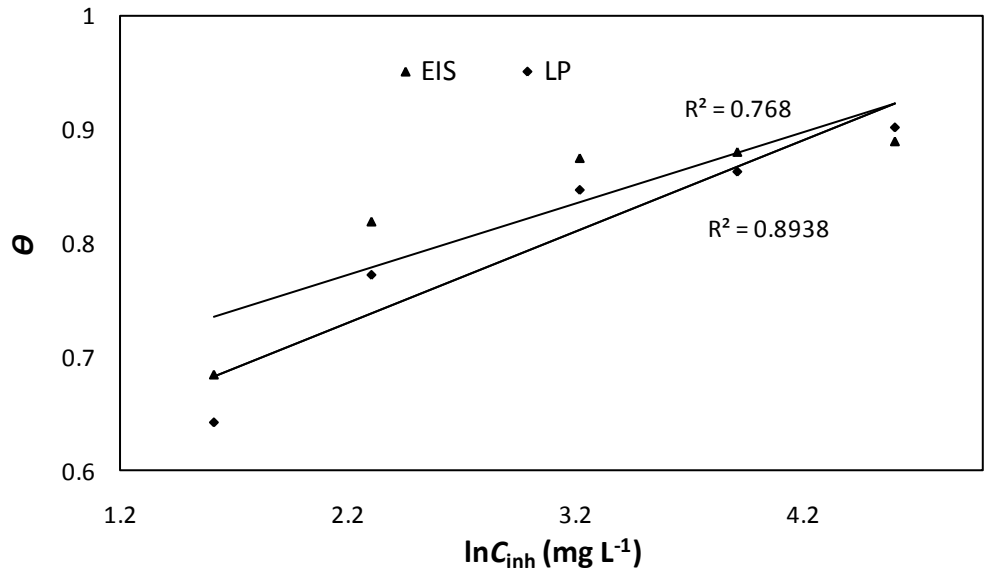

Figure 8. Temkin adsorption plots for C38 steel in 1 M HCl containing different concentrations of AEPG.

4. CONCLUSION

The alkaloids extract from *Palicourea guianensis* plant acted as an efficient corrosion inhibitor in 1 M HCl. Polarization studies showed that *Palicourea guianensis* extract was mixed-type inhibitor and its inhibition efficiency increased with the inhibitor concentration. The protection efficiency of the extract, calculated from EIS, was found also to increase with increase in concentration of the inhibitor showing a maximum efficiency of 89% at 100 mg L^{-1}. Adsorption models Langmuir, Temkin and Frunkin isotherms were tested graphically for the data and the best fit was obtained with the Langmuir isotherm. The inhibitory effect observed in polarization curves and electrochemical impedance studies results likely occurs via the adsorption of the alkaloid compounds present in the AEPG onto the steel surface.

ACKNOWLEDGEMENT
This work was supported by European Union through DEGRAD framework (FEDER funds, PRESAGE 30070).

References

1. N.O. Eddy, E. E. Ebenso, *Int. J. Electrochem. Sci.* 5 (2010) 731.
2. N. Labjar, M. Lebrini, F. Bentiss, N. Chihib, S. El-Hajjaji, C. Jama, *Mater. Chem. Phys*. 119 (2010) 330.
3. B.M. Praveen, T.V. Venkatesha, *Int. J. Electrochem. Sci.* 4 (2009) 267.
4. M.G. Hosseini, M.R. Arshadi, *Int. J. Electrochem. Sci.* 4 (2009) 1339.
5. O.K. Abiola, J.O.E. Otaigbe, *Int. J. Electrochem. Sci.* 3 (2008) 191.
6. S.A.Abd El–Maksoud, *Int. J. Electrochem. Sci.* 3 (2008) 528.
7. M. Lebrini, F. Robert, H. Vezin, C. Roos, *Corros. Sci*. 52 (2010) 3367.
8. P.C. Okafor, E.E. Ebenso, U.J. Ekpe, *Int. J. Electrochem. Sci.* 5 (2010) 978.
9. I.B. Obot, N.O. Obi-Egbedi, S.A. Umoren, E.E. Ebenso, *Int. J. Electrochem. Sci.* 5 (2010) 994.
10. M. Dahmani, A. Et-Touhami, S.S. Al-Deyab, B. Hammouti, A. Bouyanzer, *Int. J. Electrochem. Sci.* 5 (2010) 1060.
11. M. Lebrini, F. Robert, C. Roos, *Int. J. Electrochem. Sci.* 5 (2010) 1698.
12. M. Lebrini, F. Robert, A. Lecante, C. Roos, *Corros. Sci*. 53 (2011) 687.
13. L. Vrsalovic, M. Kliškic, S. Gudic *Int. J. Electrochem. Sci.* 4 (2009) 1568.
14. I.B. Obot, N.O. Obi-Egbedi, *Int. J. Electrochem. Sci.* 4 (2009) 1277.
15. E.A. Noor, *Int. J. Electrochem. Sci.* 2 (2007) 996.
16. A.M. Abdel-Gaber, B.A. Abd-El-Nabey, M. Saadawy, *Corros. Sci*. 51 (2009) 1038.
17. J.C. da Rocha, J.A. da Cunha Ponciano Gomes, E. D'Elia, *Corros. Sci.* 52 (2010) 2341.
18. R. Kanojia, G. Singh, *Surf. Eng*. 21 (2005) 180.
19. A.K. Satapathy, G. Gunasekaran, S.C. Sahoo, Kumar Amit, P.V. Rodrigues, *Corros. Sci*. 51 (2009) 2848.
20. A. Ostovari, S.M. Hoseinieh, M. Peikari, S.R. Shadizadeh, S.J. Hashemi, *Corros. Sci.* 51 (2009)1935.
21. J. Bruneton, *pharmacognosie-phytochimie, plantes médicinales*, 4ème édition, revue et augmenté, Tec&Doc-Edition Médicinales Internationales Paris, 2009, 1288 p. (ISBN. 978-2-7430-1188-8).
22. Z.B. Stoynov, B.M. Grafov, B. Savova-Stoynova, V.V. Elkin, Electrochemical Impedance, Nauka, Moscow, 1991.

23. F.B. Growcock, R.J. Jasinski, *J. Electrochem. Soc.* 136 (1989) 2310.
24. G. Reinhard, U. Rammelt, in: Proc. 6th European Symposium on Corrosion Inhibitors, Ann. Univ. Ferrara, 1985, p. 831.
25. P. Li, J.Y. Lin, K.L. Tan, J.Y. Lee, *Electrochim. Acta* 42 (1997) 605.
26. D.A. Lopez, S.N. Simison, S.R. de Sanchez, *Electrochim. Acta* 48 (2003) 845.
27. K. Jütner, *Electrochim. Acta* 10 (1990) 1501.
28. S. Martinez, M. Metikos-Hukovic, *J. Appl. Electrochem*. 33 (2003) 1137.
29. X. Wu, H. Ma, S. Chen, Z. Xu, A. Sui, *J. Electrochem. Soc*. 146 (1999) 1847.
30. H. Ma, X. Cheng, G. Li, S. Chen, Z. Quan, S. Zhao, L. Niu, *Corros. Sci.* 42 (2000) 1669.
31. L.R. Chauhan, G. Gunasekaran, *Corros. Sci.* 49 (2007) 1143.
32. R.Saratha, N.Kasthuri, P.Thilagavathy, *Der Pharma Chemica* 1 (2009) 249.
33. A.M. Abdel-Gaber, B.A. Abd-El-Nabey, I.M. Sidahmed, A.M. El-Zayady, M. Saadawy, *Corros. Sci.* 48 (2006) 2765.
34. N. O. Eddy, S. A. Odoemelam, A. O. Odiongenyi, *J Appl Electrochem* 39 (2009) 849.
35. H.A. Sorkhabi, B. Shaabani, D. Seifzadeh, *Electrochim. Acta* 50 (2005) 3446.
36. K.F. Khaled, N. Hackerman, *Electrochim. Acta* 48 (2003) 2715.
37. I. V. Aoki, I. C. Guedes, S. L. A. Maranhão. *J. Appl. Electrochem*. 32 (2002) 915.
38. B.C. Jain, J.N. Gaur, *J. Electrochem. Soc. India* 27 (1978) 165.